

# Electrical Conductivity and Vapor-Sensing Properties of $\omega$ -(3-Thienyl)alkanethiol-Protected Gold Nanoparticle Films

Heejoon Ahn,<sup>†</sup> Amol Chandekar,<sup>†</sup> Bongwoo Kang,<sup>‡</sup> Changmo Sung,<sup>‡</sup> and James E. Whitten<sup>\*,†</sup>

Departments of Chemistry and Chemical and Nuclear Engineering and Center for Advanced Materials, The University of Massachusetts Lowell, Lowell, Massachusetts 01854-5047

Received February 9, 2004. Revised Manuscript Received June 14, 2004

Gold nanoparticles protected with thiophene-terminated alkanethiols having different alkane chain lengths have been synthesized, and vapor-sensing properties of their spin-coated films have been investigated. Transmission electron microscopy and measurement of the sulfur and gold peak areas of the films by X-ray photoelectron spectroscopy indicate gold core diameters in the 3–5-nm range. Exposure of the films to chloroform, toluene, hexane, and ethanol vapors results in significant and selective increases in electrical resistance, with the response to the vapors having the following order: toluene > chloroform > hexane  $\gg$  ethanol. The magnitude of the maximum resistance change correlates well with solubility properties of the protected gold nanoparticles, as determined by optical absorbance spectroscopy and the energy of the gold plasmon. The detection sensitivity of the films increases with increasing alkanethiol chain length. These data are consistent with a sensing mechanism in which organic vapors cause swelling of the nanoparticle film, resulting in increased distance between the gold cores. In the case of ethanol, a decrease in resistance occurs at high vapor concentration, presumably due to an increase in the dielectric constant of the medium between the cores.

## Introduction

A chemiresistor-type vapor sensor is a thin-film device based on electrical conductivity changes caused by exposure to chemical vapors. The origins of the organic chemiresistor sensor can be traced to the work of Bott and Jones<sup>1</sup> who demonstrated NO<sub>2</sub> vapor sensing using a semiconducting lead-substituted phthalocyanine film as a transducer and, even earlier, to seminal studies by Rosenberg et al.<sup>2</sup> on the effect of various gases on the semiconducting properties of carotenoids. Organic semiconducting polymer sensors appeared in the 1990s and are attractive because of their ease of fabrication, low power consumption, performance over a wide temperature range, and sensitivity.<sup>3</sup> More recently, Wohltjen and Snow reported a fundamentally new type of chemiresistor sensor using alkanethiol-protected gold nanoparticles as a thin film transducer.<sup>4</sup> In the case of organic semiconducting sensors, interaction of chemical vapors with the organic film involves transfer of electrons through the conduction band.<sup>3</sup> However, in the case of the alkanethiol-protected gold nanoparticle film sensors,

the mechanism of charge transport in the sensor is believed to be electron tunneling between metal cores and electron hopping along the alkanethiolate chains.<sup>4,5</sup> The sorption of chemical vapors into the organic monolayer causes it to swell and results in an increase in the distance between metal particle cores. Consequently, the tunneling current through the metal cores and electron hopping between the alkanethiolate chains decrease upon exposure to organic vapors.

Alkanethiols have been widely used as ligands to form monolayer-protected gold nanoparticles because of their ease of synthesis and stability.<sup>6,7</sup> Vapor sensors composed of monolayer-protected gold nanoparticle films show excellent sensitivity, reversibility, selectivity, and fast response.<sup>4,8–11</sup> The high sensitivity of this type of sensor is due to its large surface area arising from

\* Corresponding author. Phone: (978)934-3666. Fax: (978)934-3013. E-mail: James\_Whitten@uml.edu.

<sup>†</sup> Department of Chemistry and Center for Advanced Materials.

<sup>‡</sup> Department of Chemical and Nuclear Engineering and Center for Advanced Materials.

(1) Bott, B.; Jones, T. A. *Sens. Actuators* **1984**, *5*, 43.

(2) Rosenberg, B.; Misra, T. N.; Switzer, R. *Nature* **1968**, *217*, 423.

(3) Bailey, R. A.; Persaud, K. C. Sensing volatile chemicals using conducting polymer arrays. In *Polymer Sensors and Actuators*; Osada, Y., DeRossi, D. E., Eds.; Springer-Verlag: Berlin, 2000; pp 149–181.

(4) Wohltjen, H.; Snow, A. W. *Anal. Chem.* **1998**, *70*, 2856.

(5) Wuelfing, W. P.; Green, S. J.; Pietron, J. J.; Cliffel, D. E.; Murray, R. W. *J. Am. Chem. Soc.* **2000**, *122*, 11465.

(6) Brust, M.; Walker, M.; Bethell, D.; Schiffrin, D. J.; Whyman, R. *J. Chem. Soc., Chem. Commun.* **1994**, 801.

(7) Terrill, R. H.; Postlethwaite, T. A.; Chen, C.-H.; Poon, C.-D.; Terzis, A.; Chen, A.; Hutchison, J. E.; Clark, M. R.; Wignall, G.; Londono, J. D.; Superfine, R.; Falvo, M.; Johnson, C. S., Jr.; Samulski, E. T.; Murray, R. W. *J. Am. Chem. Soc.* **1995**, *117*, 12537.

(8) Grate, J. W.; Nelson, D. A.; Skaggs, R. *Anal. Chem.* **2003**, *75*, 1868.

(9) Joseph, Y.; Besnard, I.; Rosenberger, M.; Guse, B.; Nothofer, H.-G.; Wessels, J. M.; Wild, U.; Knop-Gericke, A.; Su, D.; Schloegl, R.; Yasuda, A.; Vossmeier, T. *J. Phys. Chem. B* **2003**, *107*, 7406.

(10) Han, L.; Daniel, D. R.; Maye, M. M.; Zhong, C.-J. *Anal. Chem.* **2001**, *73*, 4441.

(11) Snow, A. W.; Wohltjen, H.; Jarvis, N. L. MIM Chemical Vapor Microsensors. In *2002 NRL Review*; Bultman, J. D., Ed.; Naval Research Laboratory: Washington, D.C., 2002; pp 45–55. This is also available at <http://www.nrl.navy.mil/content.php?P=02REVIEW45>.

adsorption on nanometer-size gold particles. In principle, chemical selectivity can be achieved by modifying the adsorbed alkanethiol and constructing a chemical sensor comprised of several different types of functionalized alkanethiol films, each sensitive to a varying degree to different analytes. Chemically selective sensors have also been prepared from composites of conducting carbon black and insulating organic polymers<sup>12</sup> and via layer-by-layer assembly of gold nanoparticle-dendrimer composites.<sup>13–15</sup> However, in the case of alkanethiol-protected gold nanoparticle sensors, only a handful of studies have been performed to explore the use of functionalized alkanethiols.<sup>8,10,11,16–18</sup>

Key issues impacting the sensor performance of organic-coated gold nanoparticle films include the dimensions of the gold cores and the chemical functionality and thickness of the molecular films comprising their coating.<sup>11</sup> The dimensions of the gold cores are determined by the synthetic conditions during particle growth, and the organic layer thickness is determined by the length and adsorption geometry of the alkanethiol. Optimum gold nanoparticle diameters appear to be in the 1–5-nm range,<sup>11</sup> and it is critical that neighboring gold particles not coalesce and fuse.<sup>18</sup> In addition to imparting selectivity due to its chemical functionality, the organic layer must remain intact and well-ordered to prevent coalescence of the particles. It is also important that the organic layer be thick enough to solvate the vapor to be detected, but not so thick that a lack of sensitivity is realized as a result of a relatively small change in the distances between the gold particles.

In the present study, we report for the first time the synthesis, characterization, and solvation and sensor properties of gold nanoparticles protected with thiophene-terminated alkanethiols. The goals of this work are to investigate the chemical selectivity and sensitivity of the thiophene-terminated alkanethiol-protected gold nanoparticle films and to study the effects of alkanethiol chain length on conductivity and vapor-sensing properties. The synthesis and self-assembly on macroscopic gold surfaces of thiophene-terminated alkanethiols, Th-(CH<sub>2</sub>)<sub>n</sub>-SH (Th = 3-thiophene) with  $n = 2, 6, \text{ and } 12$ , have been described in our previous work.<sup>19</sup> It was found that the  $\omega$ -(3-thienyl)alkanethiols assembled on gold surfaces with the thiophene groups at the periphery of the monolayer and that longer alkane chains gave better ordered monolayers.

## Experimental Section

**Materials.** All chemicals used in the syntheses and the chemicals used for vapor-sensing studies were purchased from Aldrich and used as received.

(12) Tillman, E. S.; Koscho, M. E.; Grubbs, R. H.; Lewis, N. S. *Anal. Chem.* **2003**, *75*, 1748.

(13) Vossmeier, T.; Guse, B.; Besnard, I.; Bauer, R. E.; Müllen, K.; Yasuda, A. *Adv. Mater.* **2002**, *14*, 238.

(14) Krasteva, N.; Besnard, I.; Guse, B.; Bauer, R. E.; Müllen, K.; Yasuda, A.; Vossmeier, T. *Nano Lett.* **2002**, *2*, 551.

(15) Krasteva, N.; Krustev, R.; Yasuda, A.; Vossmeier, T. *Langmuir* **2003**, *19*, 7754.

(16) Zamborini, F. P.; Leopold, M. C.; Hicks, J. F.; Kulesza, P. J.; Malik, M. A.; Murray, R. W. *J. Am. Chem. Soc.* **2002**, *124*, 8958.

(17) Evans, S. D.; Johnson, S. R.; Cheng, Y. L.; Shen, T. *J. Mater. Chem.* **2000**, *10*, 183.

(18) Briglin, S. M.; Gao, T.; Lewis, N. S. *Langmuir* **2004**, *20*, 299.

(19) Ahn, H.; Kim, M.; Sandman, D. J.; Whitten, J. E. *Langmuir* **2003**, *19*, 5303.

**Synthesis of Thiophene-Terminated Alkanethiol-Protected Gold Nanoparticles.** The synthesis of the thiophene-functionalized gold nanoparticles has been performed by modifying Brust's method<sup>6</sup> through the use of  $\omega$ -(3-thienyl)alkanethiols. Briefly, gold chloride (HAuCl<sub>4</sub>) is transferred by a phase-transfer reagent into a toluene solution of the  $\omega$ -(3-thienyl)alkanethiol and is subsequently reduced by adding aqueous sodium borohydride (NaBH<sub>4</sub>). As neutral gold particles nucleate and begin to grow competitively, the  $\omega$ -(3-thienyl)alkanethiol reacts with the neutral gold surfaces to form gold-sulfur thiolate bonds. Particle growth is terminated when their surfaces are completely covered by a monolayer of the  $\omega$ -(3-thienyl)alkanethiols. For abbreviation, 12-(3-thienyl)dodecanethiol-, 6-(3-thienyl)hexanethiol-, and 2-(3-thienyl)ethanethiol-protected gold nanoparticles are hereafter referred to as ThC12SAu, ThC6SAu, and ThC2SAu, respectively.

**X-ray Photoelectron Spectroscopy (XPS).** XPS measurements have been performed in a VG ESCALAB MK II photoelectron spectrometer having base pressures in the low 10<sup>-10</sup> mbar range. It is equipped with a Mg K $\alpha$  X-ray source ( $h\nu = 1253.6$  eV) and a concentric hemispherical analyzer operating in constant pass energy mode and detecting photoelectrons approximately normal to the sample plane. For the XPS measurements, gold nanoparticle films have been spin-cast from 1 mg/mL chloroform solutions onto indium tin oxide (ITO) coated substrates with areas of ca. 1 cm<sup>2</sup>.

**Transmission Electron Microscopy (TEM).** TEM studies have been performed using a Philips EM 400t microscope fitted with a LaB<sub>6</sub> filament at 120 keV. The gold nanoparticle films have been deposited onto a carbon-coated copper grid by drop-casting from a 0.1 mg/mL chloroform solution. Particle size distributions have been analyzed by digitizing the TEM micrographs with Scion image software.

**UV-Vis Spectroscopy.** UV-Vis absorbance spectra have been acquired using a Lambda 1806 spectrometer.

**Electrical Conductivity and Chemical Vapor Sensitivity.** The electrical conductivity of the functionalized gold nanoparticle films has been measured by spin-coating onto interdigitated array (IDA) microelectrodes (Microsensor Systems, Inc. Part No. M1450110) and measuring the current flow through the film at a fixed voltage at room temperature. This IDA microelectrode is composed of 50 pairs of gold electrode digits (fingers) deposited onto a quartz substrate with the following dimensions: 15- $\mu\text{m}$  electrode width, 15- $\mu\text{m}$  spacing, 4800- $\mu\text{m}$  overlapping length, and 1500- $\text{\AA}$  electrode thickness. The conductivity,  $\sigma$ , can be calculated by the following equation,<sup>20,21</sup>

$$\sigma = \frac{d \times I}{(2n - 1) \times L \times h \times V} \quad (1)$$

where  $d$  is the electrode spacing,  $I$  is the current,  $n$  is the number of electrode digits,  $L$  is the overlapping length of the electrodes,  $h$  is the film thickness, and  $V$  is the bias voltage. This equation is valid for cases in which the thickness of the films does not exceed that of the gold electrodes, as in the present study. For the results reported here, a dc voltage of 2.0 V was used. Ohmic behavior was observed in this voltage range, and the  $I$ - $V$  curve passed through the origin, within the noise of the experiment.

The chemical vapor-sensing properties of the gold nanoparticle films have been examined by exposing the IDA microelectrode films to organic vapors and measuring the electrical resistance changes of the films. Toluene, chloroform, ethanol, and hexane vapors of varying concentration were generated by bubbling dry nitrogen gas through the solvent of interest and mixing the saturated nitrogen gas with pure dry nitrogen. Concentrations are calculated from the partial pressure of the saturated vapor at room temperature. All films show very fast response to the organic vapors and complete reversibility. Upon exposure, 90% of the maximum response is reached

(20) Snow, A. W.; Wohltjen, H. *Chem. Mater.* **1998**, *10*, 947.

(21) Snow, A. W.; Barger, W. R.; Klusty, M.; Wohltjen, H.; Jarvis, N. L. *Langmuir* **1986**, *2*, 513.

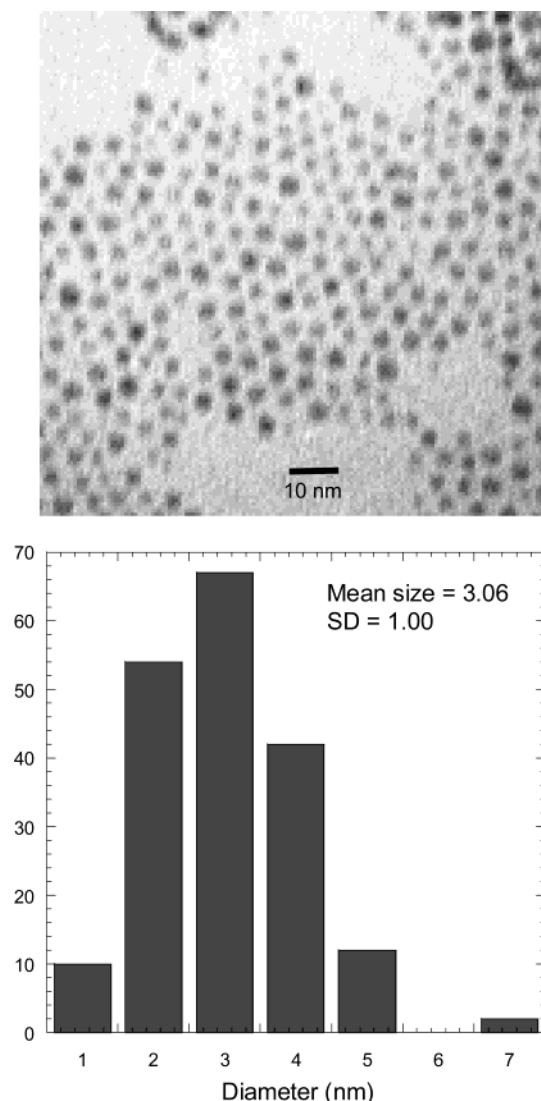


**Figure 1.** TEM micrograph of a drop-cast film of 12-(3-thienyl)dodecanethiol-protected gold nanoparticles and its size histogram.

within 3–4 s. The resistance returns to its initial value when exposure to the organic vapor is terminated by closing the bubbler. The typical overall drift in the experiment is less than 10%, even after a couple of hours. However, we have observed changes in the electrical properties of the films due to long-term storage in air.

## Results and Discussion

The size distributions of the functionalized gold nanoparticles have been characterized by transmission electron microscopy (TEM). Figure 1 shows a representative TEM micrograph of a ThC12SAu sample and its size histogram. Similar analyses were performed for ThC6SAu and ThC2SAu, and Table 1 contains mean core size and standard deviation data of the  $\omega$ -(3-thienyl)alkanethiol-protected gold nanoparticles. ThC12SAu, ThC6SAu, and ThC2SAu have mean sizes of 3.06, 2.72, and 3.13 nm, respectively, with standard deviations (SDs) of 1.00, 0.59, and 1.04 nm. The chemical compositions of the functionalized gold nanoparticle films have been analyzed using X-ray photoelectron spectroscopy (XPS), and their atomic Au/S ratios are included in Table 1. The atomic ratios were deduced from integra-

**Table 1. Characteristics of  $\omega$ -(3-Thienyl)alkanethiol-Protected Gold Nanoparticles**

	ThC2AuS	ThC6AuS	ThC12AuS
core size <sup>a</sup> (standard deviation), nm	3.13 (1.04)	2.72 (0.59)	3.06 (1.00)
Au/S <sup>b</sup>	2.2 ± 0.3	2.5 ± 0.3	2.8 ± 0.3
diameter, <sup>c</sup> nm	3.6 ± 0.6	4.2 ± 0.6	4.8 ± 0.6
thickness, <sup>d</sup> nm		5 ± 1	10 ± 1
electrical conductivity, S/cm		2.0 × 10 <sup>-5</sup>	7.8 × 10 <sup>-8</sup>

<sup>a</sup> Size was measured by TEM. <sup>b</sup> Atomic ratios were deduced from integration of XPS Au 4f and S 2p peaks with correction for their sensitivity factors. <sup>c</sup> Calculation of the diameter was based on the Au/S atomic ratios and an assumption that a spherical gold core has hexagonally close-packed gold atoms. 58.01 atoms/nm<sup>3</sup>, 13.89 atoms/nm<sup>2</sup>, and 0.66 were used for the atom density of bulk gold, the number density of surface gold atoms, and the ratio of alkanethiolates to surface gold atoms, respectively. <sup>d</sup> Thickness was measured by AFM.

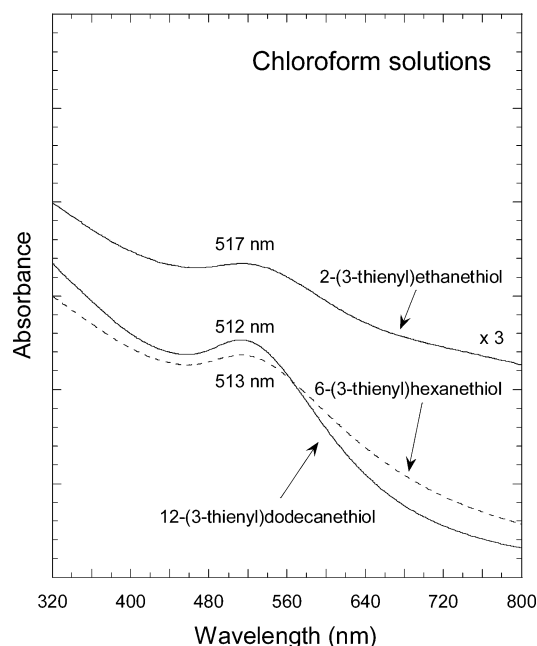


**Figure 2.** UV–Vis absorption spectra of  $\omega$ -(3-thienyl)alkanethiol-protected gold nanoparticle solutions in chloroform. The concentrations of the solutions were 0.1 mg/mL.

tion of the Au 4f and S 2p peaks with correction for their sensitivity factors.<sup>22</sup> On the basis of these atomic ratios and an assumption of spherical particles composed of hexagonally close-packed gold atoms, a model detailed by Murray and colleagues,<sup>7</sup> we calculate core diameters of 4.8 ± 0.6, 4.2 ± 0.6, and 3.6 ± 0.6 nm for ThC12SAu, ThC6SAu, and ThC2SAu, respectively. In the model, we used 58.01 atoms/nm<sup>3</sup> and 13.89 atoms/nm<sup>2</sup> and assumed a value of 0.66 for the atom density of bulk gold, the number density of surface gold atoms, and the ratio of alkanethiolates to surface gold atoms, respectively. The calculated diameters are in reasonable agreement with the results of the TEM analyses.

The optical properties of the functionalized gold nanoparticle solutions and their films have been studied with UV–Vis spectroscopy. Figure 2 shows UV–Vis spectra of the  $\omega$ -(3-thienyl)alkanethiol-protected gold nanoparticle solutions dissolved in chloroform. The spectra of ThC12SAu, ThC6SAu, and ThC2SAu solu-

(22) Scofield, J. H. *J. Electron Spectrosc. Relat. Phenom.* **1976**, *8*, 129.

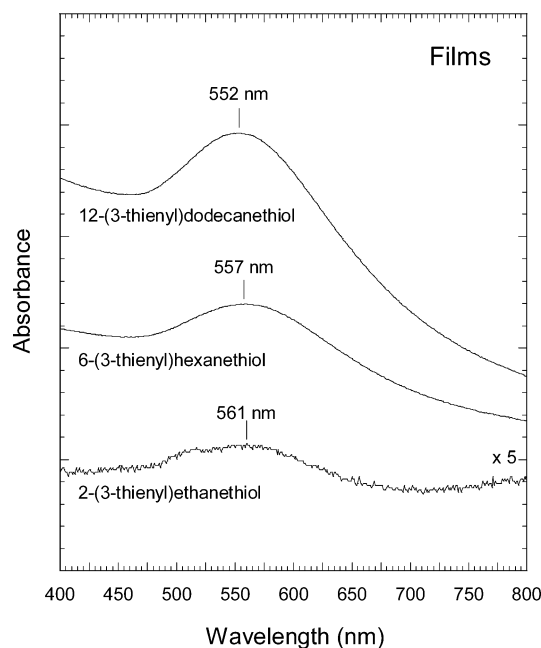


**Figure 3.** UV-Vis absorption spectra of  $\omega$ -(3-thienyl)alkanethiol-protected gold nanoparticle films spin-coated on quartz slides from 1 mg/mL chloroform solutions.

tions exhibit maximum absorption at 512, 513, and 517 nm, respectively. These absorption peaks correspond to the gold plasmon band, confirming that the solutions contain isolated nanometer-sized gold particles.<sup>23</sup> The wavelength of the maximum plasmon absorption band of the ThC2SAu solution is slightly higher than that of the ThC12SAu and ThC6SAu solutions. The red shift is caused by the slightly poorer solubility of ThC2SAu in chloroform compared to ThC12SAu and ThC6SAu. Figure 3 displays UV-Vis spectra of the three  $\omega$ -(3-thienyl)alkanethiol-protected gold nanoparticle films spin-coated onto quartz slides from 1 mg/mL chloroform solutions. When the plasmon absorption bands of solutions are compared to those of films, the plasmon bands of the films are red-shifted relative to the solutions. This red shift is due to stronger interparticle interactions caused by decreased distances between the gold nanoparticles.<sup>24</sup> The energies of the plasmon absorption bands of the films also red-shift slightly as the number of methylene units in the thiophene-terminated alkanethiols decreases. This indicates that ThC2SAu films have the strongest interparticle interactions and suggests that the thiophene-terminated alkanethiol molecules stabilize the gold particles and that the distance between the gold cores is determined by the molecular chain length of the thiophene-terminated alkanethiol. The thickness of the ThC12SAu and ThC6SAu films used for UV-Vis measurements are  $10 \pm 1$  and  $5 \pm 1$  nm, respectively. These were determined by imaging the edges of several scratches using an atomic force microscope operated in tapping mode. The thickness difference of these two gold nanoparticle films may contribute to the decrease of the maximum intensity of the plasmon peaks as the chain length decreases. In the case of ThC2SAu, the film surface was too rough to measure the thickness due to the existence of large clusters which

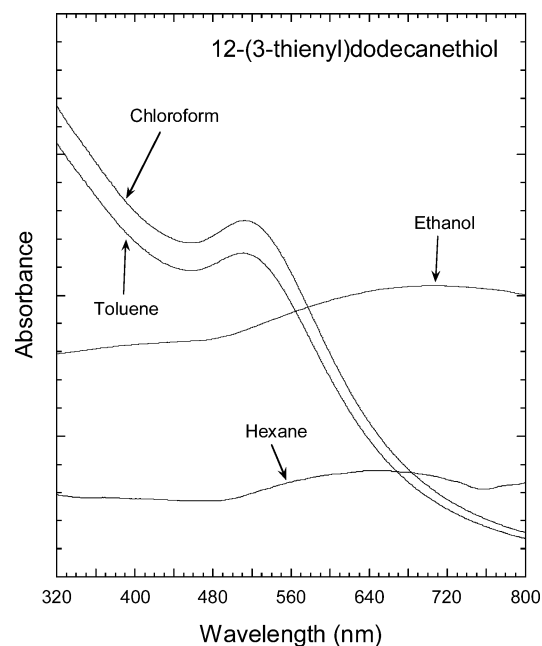


**Figure 4.** UV-Vis absorption spectra of 12-(3-thienyl)dodecanethiol-protected gold nanoparticle solutions in chloroform, toluene, hexane, and ethanol.

may be caused by poorly dissolved nanoparticles in chloroform. Figure 4 shows UV-Vis spectra of ThC12SAu solutions dissolved in chloroform, toluene, hexane, and ethanol. The functionalized gold nanoparticles are well-dissolved in chloroform and toluene, forming clear, wine-red solutions. But these particles are poorly dissolved in hexane and ethanol and easily precipitated. With respect to chloroform and toluene solutions, the plasmon absorption bands are well-pronounced at 512 nm, but the hexane and ethanol solutions show significantly broadened and red-shifted absorption peaks, with the red shifts due to poor solubility and particle agglomeration.

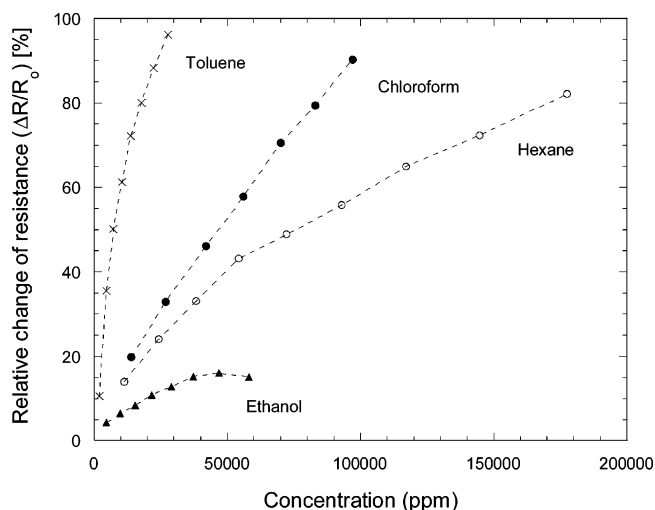
The electrical properties of the functionalized gold nanoparticle films have been measured by spin-coating onto IDA microelectrodes and measuring the current flow through the film at a fixed voltage at room temperature. Table 1 contains electrical conductivities of the nanoparticle films. Because of the high surface roughness of the ThC2SAu film and the inability to obtain an accurate film thickness measurement, the electrical conductivity of this film is unavailable. Electrical conductivities of  $2.0 \times 10^{-5}$  and  $7.8 \times 10^{-8}$  S/cm have been measured for the ThC6SAu and ThC12SAu films, respectively. The decreasing conductivity as the number of methylene units increases from 6 to 12 is due to the increased distance between gold cores as the chain length of the ligand increases.<sup>7,25</sup>

Figure 5 shows the response of the 12-(3-thienyl)dodecanethiol-protected gold nanoparticle film to toluene, chloroform, hexane, and ethanol. The response of this film to these vapors is in the following order: toluene > chloroform > hexane  $\gg$  ethanol. The varying response indicates that this nanoparticle film exhibits chemical selectivity. The responses correlate well with the solubility properties as determined by UV-Vis

(23) Mulvaney, P. *Langmuir* **1996**, *12*, 788.

(24) Quinten, M.; Kreibitz, U. *Surf. Sci.* **1986**, *172*, 557.

(25) Wuelfing, W. P.; Murray, R. W. *J. Phys. Chem. B* **2002**, *106*, 3139.



**Figure 5.** Response of the 12-(3-thienyl)dodecanethiol-protected gold nanoparticle film to various organic vapors as a function of concentration. The lines through the data are included to guide the eye.

absorption spectroscopy of their solutions in these solvents (Figure 4). Recall that the functionalized gold nanoparticles dissolve well in toluene and chloroform, consistent with the film showing the strongest responses to toluene and chloroform vapors. But the film shows weak responses to hexane and ethanol vapors, as expected from the poor solubility of the nanoparticles in these solvents. It should also be noted that, in addition to the induced morphological effect, the analyte vapor pressure also contributes inversely to the sensitivity of the film by affecting the partitioning of the analyte between the vapor and film phases, as discussed by Snow et al.<sup>11</sup>

The resistance change curves of the thiophene-functionalized gold nanoparticle films shown in Figure 5 are well-explained by the film-swelling mechanism described earlier, except for the response at high ethanol vapor concentration. In the case of ethanol, a very polar molecule, the electrical resistance of the film increases as the ethanol concentration increases, but the resistance decreases above 50 000 ppm. This type of behavior has been previously observed by Wohltjen and Snow<sup>4</sup> and explained as due to an increase in the dielectric constant of the medium surrounding the gold cores caused by absorption of polar molecules. Hence, the change in resistance is not only the result of film swelling but also the result of a change in dielectric constant of the medium between particles. As observed in Figure 5, the dielectric constant change mechanism dominates only for high vapor concentrations of polar molecules.

To investigate the effect of alkanethiol chain length on the sensitivity of the films, we have compared the responses of the three different  $\omega$ -(3-thienyl)alkanethiol-protected gold nanoparticle films to different concentrations of chloroform vapor. As shown in Figure 6, the response of the films to chloroform at a given concentration increases as the number of methylene units in the

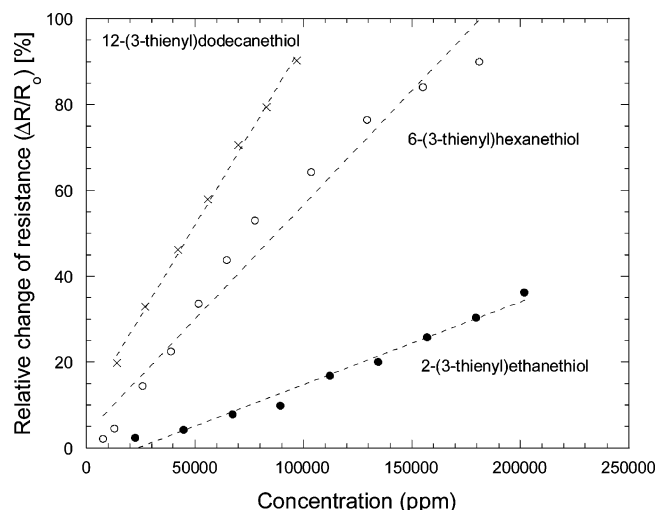


**Figure 6.** Response of  $\omega$ -(3-thienyl)alkanethiol-protected gold nanoparticle films to chloroform vapor as a function of concentration. Linear fits to the data are included.

alkanethiol chain increases. This indicates that the sensitivity of the film increases as the chain length of the ligand increases. In other words, the sensitivity of the films is significantly affected by the thickness of the monolayer covering the gold core. This behavior is related to the volume in the monolayer film in which chloroform vapors can be absorbed. As the number of methylene units increases, more organic volume is available to solvate and absorb the organic vapor. Consequently, films containing the greatest number of methylene units swell the largest amount and show the greatest vapor sensitivity, at least over the concentration range studied (ca. 1000–200000 ppm).

## Conclusions

We have synthesized thiophene-terminated alkanethiol-protected gold nanoparticles having different chain lengths in their ligands. Electrical conductivities of the 6-(3-thienyl)hexanethiol and 12-(3-thienyl)dodecanethiol-protected gold nanoparticle films are  $2.0 \times 10^{-5}$  and  $7.8 \times 10^{-8}$  S/cm, respectively. When these films are exposed to chloroform, toluene, hexane, and ethanol, the electrical resistances of the films significantly increase as the films are swelled by the vapors. The response of the sensor to the chemical vapor is governed by the solubility properties of the thiophene-terminated alkanethiols. The sensitivity of the films increases as the number of methylene units in the thiol ligand increases. Ethanol vapors cause a decrease in electrical resistance at high concentration due to the increased dielectric constant of the medium between the gold cores.

**Acknowledgment.** This material is based upon work supported by the National Science Foundation under Grant No. DMR-0089960. H. Ahn acknowledges the support of a Tripathy Memorial Graduate Fellowship.

CM049794X